Zirconium−Nitrogen Intermolecular Frustrated Lewis Pairs

Hugh B. Hamilton,† Ashley M. King,† Hazel A. Sparkes,† Natalie E. Pridmore,† and Duncan F. Wass*,‡

†School of Chemistry, University of Bristol, Cantock's Close, Bristol, BS8 1TS, United Kingdom

‡Cardiff Catalysis Institute, School of Chemistry, Cardiff University, Main Building, Park Place, Cardiff, CF10 3AT, United Kingdom

* Supporting Information

ABSTRACT: A series of intermolecular transition metal frustrated Lewis pairs (FLPs) based on zirconocene alkoxide complexes ($[Cp_2Zr(OMes)]^+$ **1** or $[Cp^*_2Zr(OMes)]^+$ **2**) with nitrogen Lewis bases (NEt_3, NEt^iPr_2, pyridine, 2-methylpyridine, 2,6-lutidine) are reported. The interaction between Zr and N depends on the specific derivatives used, in general more sterically encumbered pairs leading to a more frustrated interaction; however, DOSY NMR spectroscopy reveals these interactions to be dynamic in nature. The pairs undergo typical FLP-type reactivity with D_2, CO_2, THF, and PhCCD. The catalytic dehydrocoupling of $Me_2NH{\cdot}BH_3$ is also reported. Comparisons can be made with previous work employing phosphines as Lewis bases suggesting that hard−hard or hard−soft acid−base considerations are of little importance compared to the more prominent roles of steric bulk and basicity.

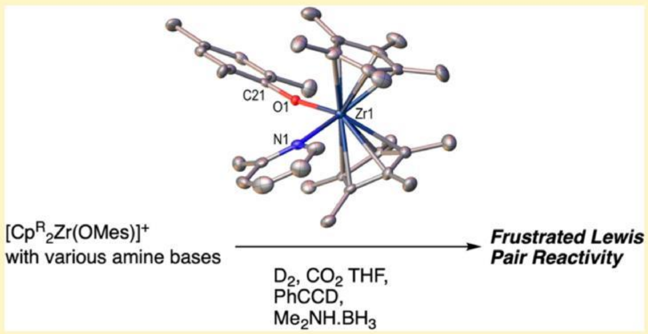

INTRODUCTION

Frustrated Lewis pairs (FLPs) first came to prominence over a decade ago,[1] and the subject area is continuing to reveal powerful new chemistry for small molecule activation and catalysis. Main group FLPs have been the focus of much of this chemistry, having been used to perform a wide variety of transformations with both inter- and intramolecular systems.[2,3] We have focused on the use of Zr(IV) cations as the Lewis acidic component in FLPs, which have predominantly taken the form of a zirconocene in combination with an intra-molecular phosphine moiety; other groups have taken a similar approach (Figure 1). The FLPs produced (A−H) have been used for the effective activation of a number of small molecules including H_2, CO_2, H_2CO, PhCCH, C_2H_4, THF, Et_2O, and Me_2CO, in addition to performing the cleavage of C−Cl and C−F bonds, and catalytic amine-borane dehydrocoupling.[4−11]

Intermolecular main group FLPs have been explored in parallel with intramolecular examples;[2] by contrast, intermolecular transition metal FLPs are far less explored with only the activation of N_2O using a Zr(IV)/P^tBu_3 FLP reported by Stephan et al. (Scheme 1),[12] and a wider exploration of intermolecular Zr(IV)/phosphine systems reported by our group in 2016 (Scheme 2).[13,14] The activation of CO_2 and H_2, along with the ring-opening of THF and activation of phenylacetylene (via both proton abstraction and 1,2-addition), by this latter system shows that these more easily modified (and less synthetically challenging) systems can achieve the same useful chemistry.

An outstanding question for Zr(IV)-based FLPs is the extent to which the hard−soft mismatch between the hard zirconocene center and the soft phosphine Lewis base influences the "frustration" of the FLP produced. Do Zr(IV)-amine pairs, in which a stronger hard−hard interaction is expected, still behave as FLPs? Amines have already been widely used in main group FLP chemistry.[15−30] An intra-molecular example (M, Figure 2) has been reported and was able to perform H activation, chloride abstraction from CH_2Cl_2, and proton[2] abstraction from phenylacetylene all well-established FLP reactions.[9] We have also reported that Zr(IV) cations catalyze the hydrogenation of imines, whereby the imine itself acts as the Lewis basic component of an FLP.[31]

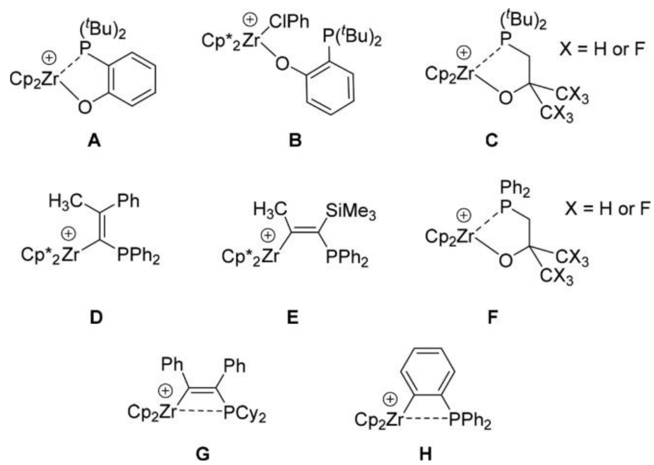

Figure 1. Intramolecular Zr/P FLPs developed by our group (A−C) and by Erker et al. (D−H). In all cases, the $[B(C_6F_5)_4]^-$ or $[MeB(C_6F_5)_3]^-$ counterion has been omitted for clarity.

Scheme 1. Intermolecular Zr/P FLP Used for N_2O Activation

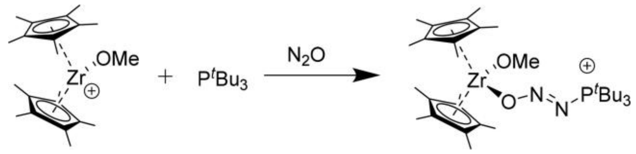

Scheme 2. Intermolecular Zr/P FLPs Developed by Our Group[a]

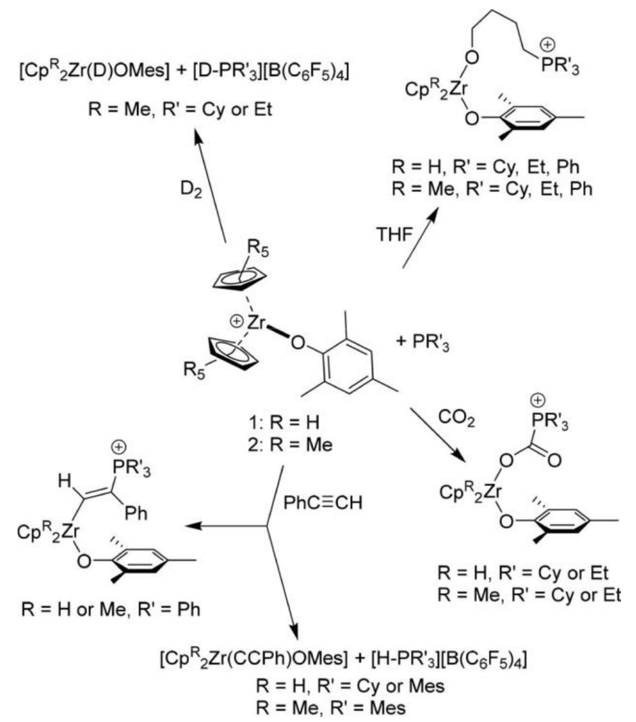

[a]$[B(C_6F_5)_4]^-$ counterion omitted for clarity.

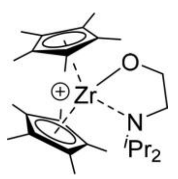

M

Figure 2. Zr/N FLP M developed by Erker et al. $[B(C_6F_5)_4]^-$ counterion omitted for clarity.

This paper demonstrates that pairs formed from zirconocenes with a wider variety of amine bases are effective and versatile FLPs.

RESULTS AND DISCUSSION

Previously, the Zr(IV) cations 1 and 2 (Figure 3) were combined with a series of phosphines in order to perform FLP-type reactions;[13] the same Zr(IV) cations were explored in a similar way with a group of nitrogen-based Lewis bases. The selection of nitrogen compounds was chosen due to the varying basicities and steric bulk of the different species, with NEt_3 (a, pK_a = 10.8) and $^iPr_2NEt$ (b, pK_a = 11.4) being more basic than pyridine (c, pK_a = 5.3) and its derivatives 2-

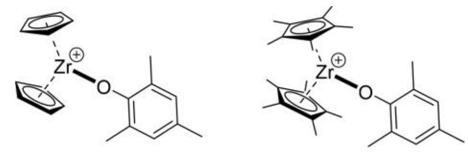

1 **2**

Figure 3. Zr(IV) cations used in this work. The $[B(C_6F_5)_4]^-$ counterions has been omitted for clarity.

methylpyridine (d, pK_a = 5.9) and 2,6-lutidine (2,6-dimethylpyridine) (e, pK_a = 6.8).[32−35]

When 1 is mixed with a−e, a lightening of the yellow solution is seen in all cases upon addition of the Lewis base. The reaction of 2 with a, b, and e resulted in a color change from orange to deep red, whereas the addition of c and d gave green and lighter orange solutions, respectively. Examining these interactions by ^{15}N NMR spectroscopy gave inconclusive results. However, by using ^{15}N-HMBC NMR spectroscopy reliable data were obtained; the results and comparison to the free Lewis base resonances are shown in Table 1. The

Table 1. ^{15}N-HMBC NMR Chemical Shifts of the Lewis Bases a−e and the Lewis Pairs 1a−e and 2a−e

Lewis base	^{15}N-HMBC NMR, δ/ppm	Zr/N	^{15}N-HMBC NMR, δ/ppm	Zr/N	^{15}N-HMBC NMR, δ/ppm
NEt_3 (a)	47.6	1a	163.5	2a	54.2
$^iPr_2NEt$ (b)	57.5	1b	185.5	2b	
C_5H_5N (c)	318.9	1c		2c	260.5
$C_5H_4(CH_3)N$ (d)	317.7	1d	302.1	2d	261.1
$C_5H_3(CH_3)_2N$ (e)	317.2	1e	249.8	2e	286.0

correlating data for 1c was unobtainable due to a very weak signal, and 2b resulted in FLP degradation and formation of $[H\text{-}N(^iPr)_2Et][B(C_6F_5)_4]$ within the time frame of the experiment. Comparing, for example, free NEt_3 (a) with 1a and 1b, it is apparent from the large change in chemical shift that a strong Lewis pair interaction results with the less bulky zirconocene 1, whereas only a small shift is observed for the bulky 2. For less basic pyridine-type bases, results are more inconclusive with the suggestion of a weaker interaction.

Diffusion-Ordered SpectroscopY (DOSY) NMR spectros-copy has proved to be a useful tool in FLP chemistry, the interaction between the Lewis acid and Lewis base being dynamic in nature, with an equilibrium between the "bound" (classical Lewis pair) and "unbound" ("frustrated" Lewis pair) states. The degree to which the equilibrium lies toward either state depends upon the specific Lewis pair, and the relative diffusion coefficients (D) of the separate components and pair are revealing. This analysis proved useful with our previous Zr/P systems,[13] indicating that some "frustration" is present even if the equilibrium lies well toward the bound pair; this was born out in the reactivity pattern observed. The diffusion coefficients (D) of the free and combined species can be seen in Table 2.

The results are somewhat surprising in that a and b have similar diffusion coefficients in the presence or absence of either zirconocene, suggesting pair-separated species predominate even though these aliphatic amines are the most basic. By contrast, pyridine-derived bases c−e have significantly smaller diffusion coefficients in the presence of 1 or 2, suggesting a

Table 2. Diffusion Coefficients (D) of the Free and Combined Lewis Pair Species, with All Results Obtained Using PhBr-d_5 at a Concentration of 0.06 mol dm^{-3}[a]

Lewis base	D of base	D of base with 1	D of base with 2	D of 1 with base	D of 2 with base
NEt_3 (a)	9.2	8.2	8.7	3.3	4.4
$^iPr_2NEt$ (b)	8.6	9.0	9.0	3.3	3.6
C_5H_5N (c)	11.8	5.7	4.0	3.3	3.3
$C_5H_4(CH_3)N$ (d)	11.0	5.2	5.2	2.5	2.3
$C_5H_3(CH_3)_2N$ (e)	9.7	6.8	6.8	2.3	2.1

[a]All values have units of $\times 10^{-10}$ m^2 s^{-1}. D of 1 in absence of base is 6.0×10^{-10} m^2 s^{-1}. D of 2 in absence of base is 8.6×10^{-10} m^2 s^{-1}.

more persistent interaction. A possible explanation is the more planar geometry of c−e facilitating a minimization of steric clash in comparison to the more three-dimensional a and b. It is also noteworthy that 1 and 2, despite significant steric differences, show similar results. This is in contrast to similar experiments with phosphine bases where the less sterically encumbered 1 showed a marked tendency to form less dynamic pairs.

Single crystals of 2c and 2d suitable for X-ray diffraction study were obtained, and the solid-state structures of 2c and 2d are shown in Figure 4. 2c possesses a shorter Zr−N bond

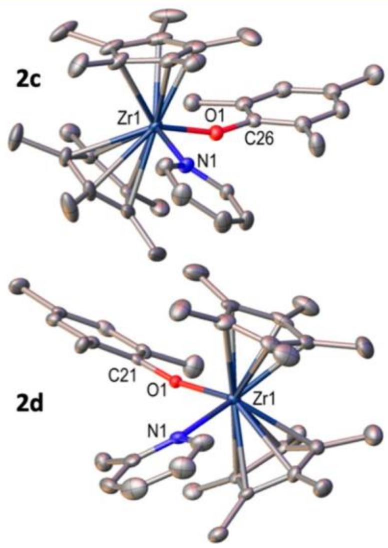

Figure 4. Molecular structures of 2c (top) and 2d (bottom), as determined by single crystal X-ray diffraction. Thermal ellipsoids are drawn at the 50% probability level. Hydrogen atoms, the $[B(C_6F_5)_4]^-$ counterion, and PhCl solvent of crystallization are omitted for clarity. Selected bond lengths (Å) and angles (deg): 2c: Zr1−O1 1.982(2), Zr1−N1 2.326(3), O1−C26 1.375(4), Zr1−O1−C26 158.8(2), Cp*−Zr−Cp* 135.5(7). 2d: Zr1−O1 1.975(3), Zr1−N1 2.386(4), O1−C21 1.369(5), Zr1−O1−C21 167.4(3), Cp*−Zr−Cp* 132.7(9).

(2.326(3) Å) than 2d (2.386(4) Å), likely a result of the increased steric bulk of d. Complex 2c also has greater bending of the alkoxide fragment (bond angle Zr1 O1 C26 158.8(2)°) compared to 2d (Zr1 O1 C21 167.4(3)°); in 2, this angle is almost completely linear (176.7(2)°). While it is tempting to rationalize this effect in terms of the multiple bond character between the Zr and O atoms changing according to other donor ligands, alkoxide bond angles are known to be an unreliable indicator of such effects, and a steric rationale is also possible.[13]

Reactivity of Lewis Pairs with Dihydrogen (D_2). Initial investigations into the ability of these Zr/N systems to activate small molecules involved reactions with dihydrogen. D_2 was used in place of H_2 to allow for easier reaction monitoring via ^2H NMR spectroscopy.

For 1a−e, no reaction was observed upon addition of D_2 gas (1 bar) to a PhCl solution of the pair (Scheme 3). This is in line with previous work where at least one Cp* ligand was necessary for the reaction to proceed[4] and adds credence to the hypothesis that transient binding of H_2 to the Zr center is required for subsequent activation to occur, meaning that simply changing the Lewis base from a phosphine to a nitrogen compound does not seem to have any effect.

The reaction proceeded smoothly for Lewis pairs 2a, 2b, and 2e with the characteristic Zr-D singlet appearing in the ^2H NMR spectra for each reaction (δ = 6.06 ppm) by the time spectra were recorded (less than 1 min). For 2a and 2b the ^2H resonance for the ammonium salts was not seen, as these compounds are insoluble in PhCl. For 2e, a broad resonance is seen at 12.4 ppm in the ^2H spectrum, corresponding to the $[C_5H_3(CH_3)_2N\text{-}D]^+$ species.

Neither the 2c nor 2d pairs demonstrated reactivity toward D_2, likely a result of the lower basicity of the Lewis bases, in addition to the more persistent Zr−N interactions as evidenced by DOSY NMR studies.

Reactivity of Lewis Pairs with Carbon Dioxide. PhBr-d_5 solutions of the Lewis pairs 1a−e and 2a−e were exposed to 1 bar CO_2 (Scheme 4). The pairs 1a and 1b reacted almost instantly, with both turning much paler yellow. ^{15}N-HMBC NMR spectra showed new peaks at 446.0 and 446.5 ppm respectively, which were assigned to the CO_2 activated product. No reaction was seen for 1c; however, both 1d and 1e reacted, albeit more slowly than 1a and 1b (<20 min), with the signals at 450.1 and 464.0 ppm respectively in the ^{15}N-HMBC NMR spectra.

Upon addition of CO_2, 2a instantly changed color to yellow, with the new resonance in the ^{15}N-HMBC NMR spectrum (δ = 343.3 ppm) assigned to the CO_2 activation product. In the case of 2b a signal in the ^{15}N-HMBC NMR spectrum could not be obtained, and although a color change suggests reaction, further analysis proved inconclusive. Reactions were also seen for both 2d and 2e, with the CO_2 activation products assigned in the ^{15}N-HMBC NMR (2d: δ = 438.1 ppm, 2e: δ = 466.1 ppm). Compound 2c was found to be inactive for CO_2 activation.

Reactivity of Lewis Pairs with Tetrahydrofuran (THF). The FLP systems were also tested for their ability to ring-open tetrahydrofuran (THF), with bromobenzene-d_5 solutions of 1a, 1b, 1d, and 1e undergoing a rapid color change to a bright yellow solution upon addition of THF indicating formation of the Zr-THF adduct (Scheme 5). Formation of the ring-opened products then followed, with the quickest reaction seen for 1a (24 h). No heating was required for this reaction to reach completion, although some unreacted Zr-THF adduct still remained. Heating at 80 °C for several days resulted in no further conversion. More sluggish reactivity was seen with 1d and 1e, with heating at 80 °C over 3 days required for the reactions to reach completion. 1b demonstrated much slower reactivity still, with very low conversion (20%) achieved after 3 days at 80 °C and no increase in conversion when left to heat

Scheme 3. Reactivity of Systems 1a−e and 2a−e with D_2 (1 bar)

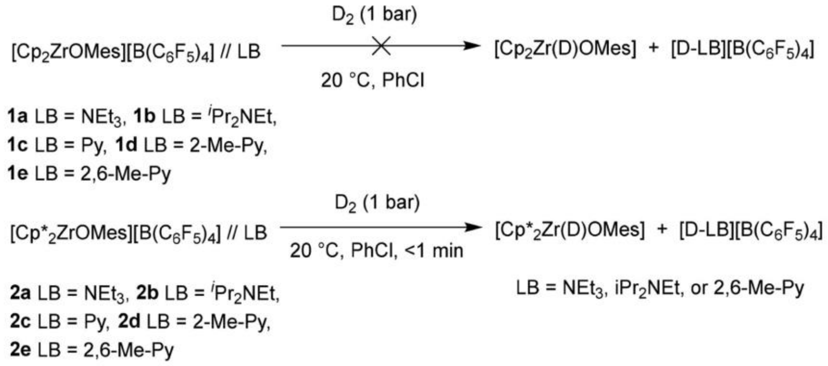

Scheme 4. Reaction of 1a−e and 2a−e with CO_2 Gas (1 bar)

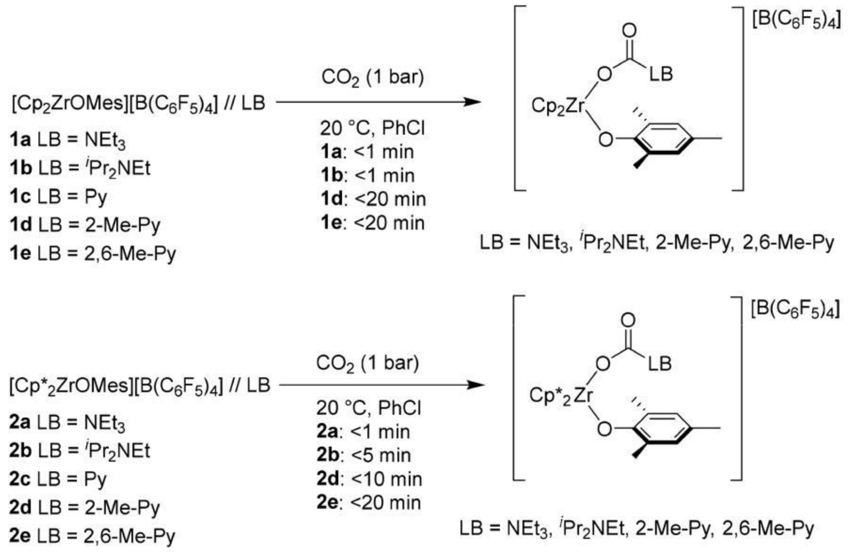

Scheme 5. Reactions of 1a−e and 2a−e with Tetrahydrofuran (THF)

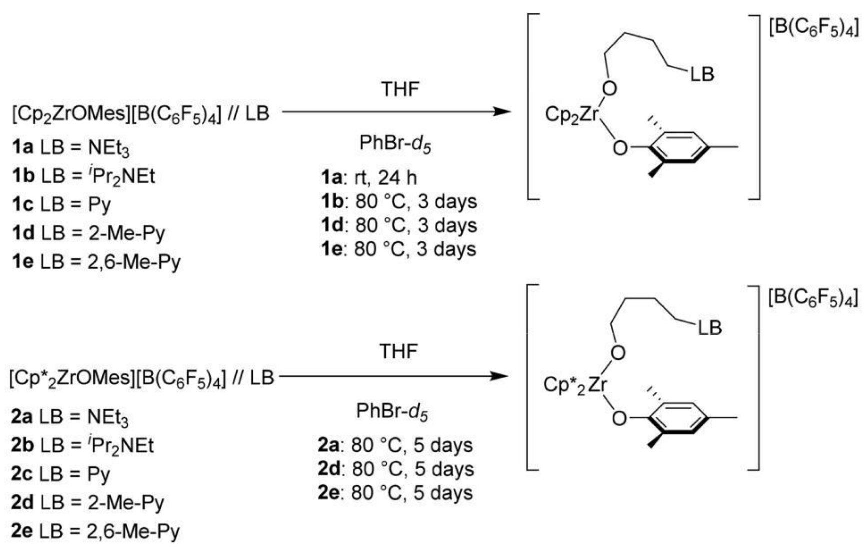

for a further 10 days. No product formed in the reaction of 1c, although the bound pyridine was eventually displaced by the THF after several days of heating at 80 °C.

Successful reactivity was also seen with 2a, 2d, and 2e, although all of these reactions required much longer timeframes than their Cp counterparts, with 5 days of heating at 80 °C required for the reactions to reach completion. Surprisingly, 2d was the most reactive of these three samples, achieving the highest yield of 40% (by NMR). 2a and 2e had very low yields of 17% and 7% respectively (by NMR), which may be a result of their higher steric bulk being more inhibitory for this reaction when Cp* ligands are present

Scheme 6. Reaction of FLP Systems 1a−e and 2a−e with Phenylacetylene-d (PhCCD)

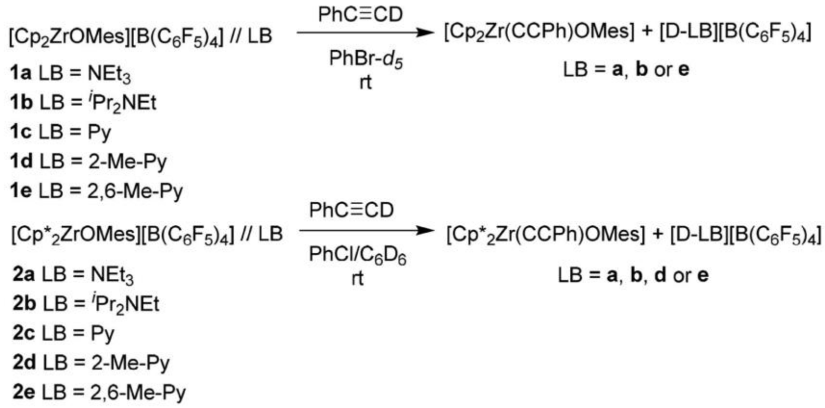

instead of Cp. The more electron-rich Cp* ligands may also result in comparatively reduced polarization/activation of the bound THF, thereby making subsequent attack from the Lewis base and consequent ring-opening less favorable.

Reactivity of Lewis Pairs with Phenylacetylene-d. Reactions of terminal alkynes with FLPs have been shown to proceed via 1,2-addition or deprotonation.[36−40] In this present case, all of the pairs 1a, 1b, 1e and 2a, 2b, 2d, 2e react with phenylacetylene-d (PhCCD), via deprotonation of the alkyne (Scheme 6). For 1a, an instant color change is seen upon addition of PhCCD (to a lighter yellow), followed by the formation of $[D\text{-}NEt_3][B(C_6F_5)_4]$ crystals after several minutes and concurrent formation of the zirconium acetylide complex. Both 1b and 1e also demonstrate formation of the $[D\text{-}{}^iPr_2NEt][B(C_6F_5)_4]$ and $[2,6\text{-Me-Py-D}][B(C_6F_5)_4]$ salts; however these reactions are more sluggish (5 and 30 min respectively). No reaction was seen for 1c and 1d. 2a, 2b, 2d, and 2e all reacted successfully with PhCCD, again yielding the deprotonation product.

Less basic, less sterically bulky phosphine Lewis bases have been shown to perform the 1,2-addition reaction previously. The results here suggest harder nitrogen bases are more likely to react via a deprotonation pathway.[13]

Catalytic Dehydrocoupling of $Me_2NH{\cdot}BH_3$. The ability of the Zr/N systems to perform catalysis was tested through the dehydrocoupling of $Me_2NH{\cdot}BH_3$. The reactions were monitored by $^{11}B\{^1H\}$ NMR spectroscopy, employing a 10 mol % catalyst loading, with the results shown in Table 3. 1a, 1e, and 2e achieved complete conversion and >95% yields within 9.5, 10.5, and 7.5 h respectively, with 2,6-dimethylpyridine the only Lewis base producing high conversions and yields with both cations.

The ability of NEt_3 to catalyze the reaction when combined with 1, but not with 2, is in line with previous work which employed phosphines as the Lewis base (P^tBu_3, PCy_3, PEt_3, PPh_3, $PMes_3$, and $P(C_6F_5)_3$).[14] The poor performance of 2a and 2b is also likely to be a result of the degradation over time; when 2 and a or b are left together in solution, the precipitation of $[H\text{-}NEt_3][B(C_6F_5)_4]$ or $[H\text{-}{}^iPr_2NEt][B(C_6F_5)_4]$ crystals is observed within a few hours. We were unable to isolate and identify the Zr complex. Increasing reaction temperature to 60 °C improved reaction rates as expected; for 1a, 1e, and 2e complete conversion was achieved within 30 min. The pairs 2c−e are surprisingly able catalysts for this reaction, outperforming previously reported Zr(IV)-phosphine FLP catalysts.

Table 3. Catalytic Dehydrocoupling of $Me_2NH{\cdot}BH_3$ using FLP systems 1a−e and 2a−e

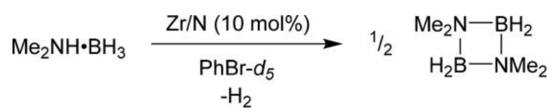

catalyst	temperature (°C)	time (h)	yield (%)	conversion (%)
1a	25	9.5	97	100
1a	60	0.45	93	100
1b	25	14	7	26
1c	25	14	0	0
1d	25	14	9	30
1e	25	7.5	79	92
1e	25	10.5	96	100
1e	25	14	98	100
1e	60	0.5	90	100
2a	25	14	9	10
2b	25	14	13	15
2c	25	14	47	47
2d	25	14	36	42
2e	25	6.5	97	100
2e	25	7.5	>99	100
2e	60	0.5	98	100

Using both basicity and steric bulk as rational predictors of reactivity is still difficult. This is highlighted by the fact that P^tBu_3 ($pK_a = 11.4$) [41] was the only phosphine (in combination with 1) shown to have reactivity similar to 1a, 1e, or 2e, whereas 1b showed very poor reactivity, despite b being more similar to P^tBu_3 in terms of basicity and steric bulk.

The mechanism of these reactions is proposed to follow the same cycle that has been previously reported,[42] with the same distribution of intermediates seen in the $^{11}B\{^1H\}$ NMR spectra during the reactions (Figure 5). Indeed, examination of the catalytic cycle gives greater clues as to the reason for the varying results seen for each catalyst. The principle role of the Lewis base in the catalytic cycle is currently understood to be the deprotonation of $Me_2NH{\cdot}BH_3$ (Scheme 7). Therefore, it may be that 1a, 1e, and 2e are more effective at both the deprotonation step and subsequent dihydrogen release. In the case of 1b, N,N-diisopropylethylamine may be too bulky to effectively deprotonate $Me_2NH{\cdot}BH_3$, and the subsequent ammonium salt may be too stable for easy dihydrogen release.

If we compare the reaction profiles for the reactions of 1a (Figure 6) and 2e (Figure 7), it is clear that a larger concentration of $Me_2NH\text{-}BH_2\text{-}Me_2N\text{-}BH_3$ is present for 1a.

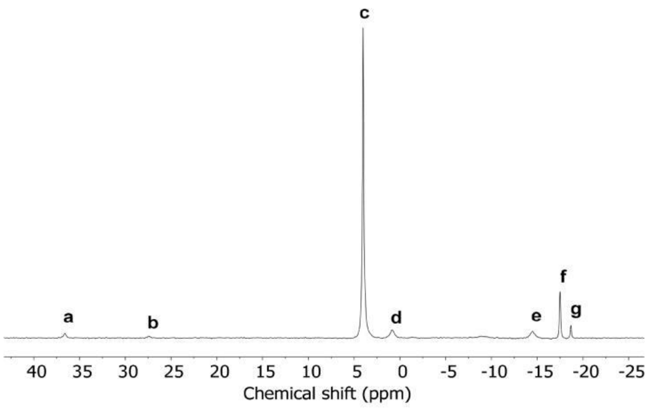

Figure 5. $^{11}B\{^{1}H\}$ NMR spectrum (160 MHz, 25 °C, PhBr-d_5, 7.5 h) for the reaction between $Me_2NH·BH_3$ and 10 mol % 2.1b. a = $Me_2N = BH_2$ (36.6 ppm), b = $HB(NMe_2)_2$ (27.5 ppm), c = $[Me_2N\text{-}BH_2]_2$ (4.03 ppm), d = $Me_2NH\text{-}BH_2\text{-}Me_2N\text{-}BH_3$ (0.82 ppm), e = $Me_2NH·BH_3$ and $Me_2NH\text{-}BH_2\text{-}Me_2N\text{-}BH_3$ (−14.5 ppm), f = $[B(C_6F_5)_4]^-$ (−17.5 ppm), g = $Me_2N(B_2H_5)$ (−18.7 ppm).

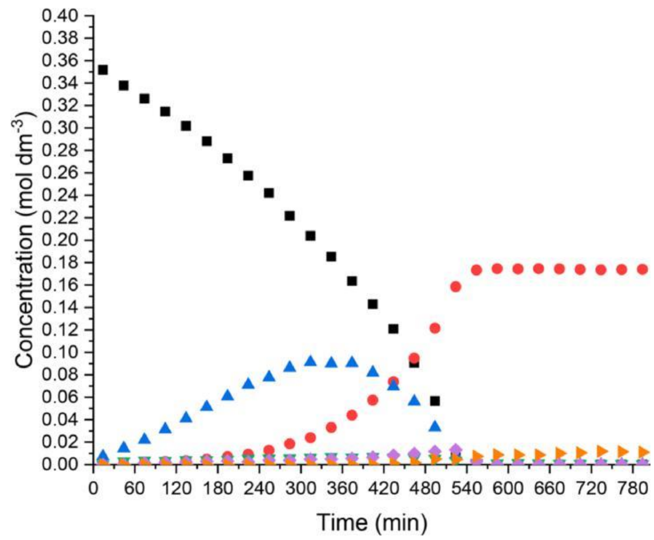

Figure 6. Reaction of 1a with $Me_2NH·BH_3$ (25 °C, PhBr-d_5, 14 h): (black ■) $Me_2NH·BH_3$; (red ●) $[Me_2N\text{-}BH_2]_2$; (blue▲) $Me_2NH\text{-}BH_2\text{-}Me_2N\text{-}BH_3$; (purple) $Me_2N = BH_2$; (green ▼) $Me_2N(B_2H_5)$; (orange triangles) $HB(NMe_2)_2$.

This is one reason for slower product formation and is perhaps a result of the persistence of the ammonium salt in the reaction which, by preventing the release of H_2 through reaction with $Cp_2Zr(H)OMes$, means there is less $[Cp_2ZrOMes]^+$ available for the conversion of $Me_2NH\text{-}BH_2\text{-}Me_2N\text{-}BH_3$, thus reducing the rate of product formation and overall catalytic turnover.

CONCLUSION

A range of intermolecular zirconium/nitrogen FLPs have been synthesized through combination of zirconocene cations with either an amine or a pyridine derivative. The nature of the Lewis acid/Lewis base interaction was elucidated through DOSY NMR spectroscopic studies, before the activation of a number of different small molecules was demonstrated. Steric effects once again play an important role, with pyridine (c) largely being shown to be an ineffective Lewis base for these reactions. The dehydrocoupling of $Me_2NH·BH_3$ was also achieved, with 2,6-dimethylpyridine and triethylamine shown to be the most effective Lewis bases. These results highlight that the hard−soft mismatch in previous intermolecular Zr(IV)-phosphine FLPs is of little or secondary importance. Given the judicious choice of nitrogen base, very similar FLP reactivity is observed in these Zr(IV)-amine systems, with steric bulk and basicity remaining the key factors in determining reactivity.

EXPERIMENTAL SECTION

General Considerations. Unless otherwise stated, all manipulations were undertaken under an atmosphere of argon or nitrogen using standard glovebox (O_2 < 0.1 ppm, H_2O < 0.1 ppm) and Schlenk line techniques. All glassware was dried in an oven at 200 °C overnight and cooled under a vacuum prior to use. The complexes $[Cp_2ZrOMes][B(C_6F_5)_4]$ and $[Cp^*_2ZrOMes][B(C_6F_5)_4]$ were synthesized following a literature procedure.[13] Triethylamine, N,N-diisopropylethylamine, pyridine, 2-methylpyridine, and 2,6-dimethylpyridine were purchased from Sigma-Aldrich and distilled from CaH_2 prior to use. $Me_2NH·BH_3$ was purchased from Sigma-Aldrich and purified by sublimation prior to use (25 °C, 2×10^{-2} Torr).

Scheme 7. Proposed Reaction Mechanism for the Catalytic Dehydrocoupling of $Me_2NH·BH_3$ Using a Zr(IV)/FLP[a]

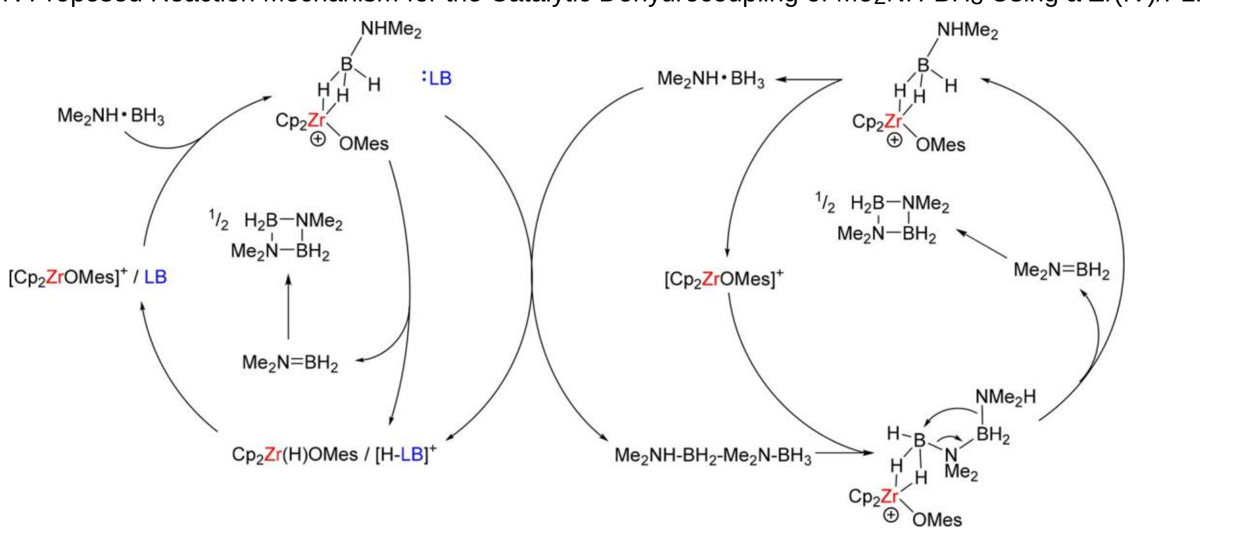

[a]The $[B(C_6F_5)_4]^-$ counterion has been omitted for clarity.

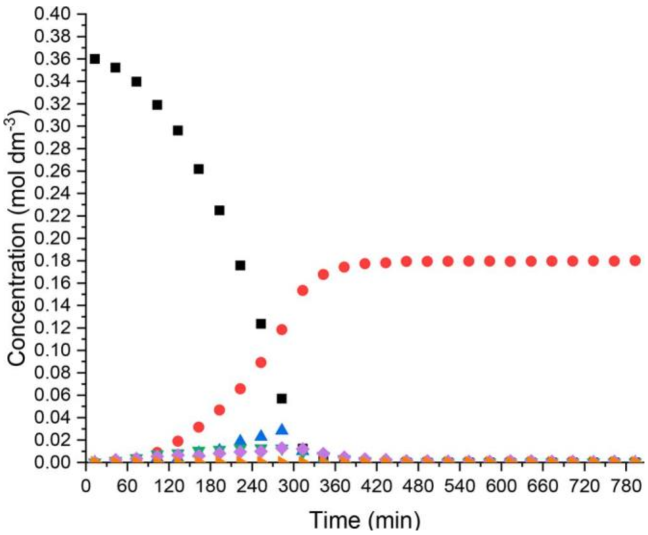

Figure 7. Reaction of 2e with $Me_2NH{\cdot}BH_3$ (25 °C, PhBr-d_5, 14 h): (black ■) $Me_2NH{\cdot}BH_3$; (red ●) $[Me_2N\text{-}BH_2]_2$; (blue▲) $Me_2NH\text{-}BH_2\text{-}Me_2N\text{-}BH_3$; (purple) $Me_2N = BH_2$; (green ▼) $Me_2N(B_2H_5)$; (orange triangles) $HB(NMe_2)_2$.

Phenylacetylene-d was purchased from Sigma-Aldrich and purified by distillation before use. Reagent gases (D_2 and CO_2) were dried prior to using by passing through a −78 °C trap. THF was purified using a Grubbs type purification system. Chlorobenzene was purchased from Sigma-Aldrich and dried over 4 Å molecular sieves prior to use.

NMR spectra were recorded using Jeol ECS 300 (300 MHz), Bruker Nano 400 (400 MHz), Jeol ECS 400 (400 MHz), Varian VNMRS500 (500 MHz), and Bruker Avance III HD 500 Cryo (500 MHz) spectrometers. ^{15}N-HMBC NMR spectra are referenced to NH_3. Deuterated solvents were obtained from Sigma-Aldrich (benzene-d_6, bromobenzene-d_5, and acetonitrile-d_3) and distilled from CaH_2 or dried over 4 Å molecular sieves prior to use. Spectra of air-sensitive compounds were recorded using NMR tubes fitted with J. Young valves. Spectra of boron-containing compounds were obtained using quartz NMR tubes fitted with J. Young valves.

X-ray diffraction experiments on 2c and 2d were carried out at 100(2) K on a Bruker APEX II diffractometer using Mo−Kα radiation (λ = 0.71073 Å). See the Supporting Information for further details.

Mass spectrometry experiments were carried out by the University of Bristol Mass Spectrometry Service on a Bruker Daltronics MicrOTOF II with a TOF analyzer or a Waters Synapt G2S with an IMS-Q-TOF analyzer. All samples were run in predried PhCl or CH_3CN.

Generation of FLPs. $[Cp_2ZrOMes][B(C_6F_5)_4]$ // LB (1a−e). In a glovebox, 1 (30 mg, 0.029 mmol) was dissolved in bromobenzene-d_5 (0.5 mL) before the Lewis base (a = NEt_3 (4.1 μL, 0.029 mmol), b = $^iPr_2NEt$ (5.1 μL, 0.029 mmol), c = pyridine (2.4 μL, 0.029 mmol), d = 2-methylpyridine (2.9 μL, 0.029 mmol), e = 2,6-dimethylpyridine (3.4 μL, 0.029 mmol)) was added. A color change (orange to yellow) was observed in each case.

The FLP was then used in situ for reactions with substrates, without isolation.

1a. ^{1}H NMR (500 MHz, PhBr-d_5) δ 6.75 (2H, s, m-ArH), 6.10 (10H, s, Cp), 2.36 (6H, q, $^3J_{HH}$ = 7.2 Hz, $N(CH_2CH_3)_3$), 2.20 (3H, s, p-Ar-CH_3), 1.86 (6H, s, o-Ar-CH_3), 0.80 (9H, t, $^3J_{HH}$ = 7.2 Hz, $N(CH_2CH_3)_3$) ppm. ^{15}N-HMBC NMR (500 MHz, 51 MHz, PhBr-d_5) δ 163.5 (Zr-NEt_3) ppm. NB: NEt_3 δ = 47.6 ppm.

1b. ^{1}H NMR (500 MHz, PhBr-d_5) δ 6.75 (2H, s, m-ArH), 6.10 (10H, s, Cp), 2.90 (2H, sept, $^3J_{HH}$ = 6.5 Hz, $N(CH(CH_3)_2)_2$), 2.37 (2H, q, $^3J_{HH}$ = 7.2 Hz, NCH_2CH_3), 2.19 (3H, s, p-Ar-CH_3), 1.86 (6H, s, o-Ar-CH_3), 1.04−0.58 (15H, br, $CH_3CH_2N(CH(CH_3)_2)_2$) ppm. ^{15}N-HMBC NMR (500 MHz, 51 MHz, PhBr-d_5) δ 185.5 (Zr-$N(^iPr)_2Et$) ppm. NB: $^iPr_2NEt$ δ = 57.5 ppm.

1c. ^{1}H NMR (500 MHz, PhBr-d_5) δ 8.19 (2H, m, o-PyH), 7.46 (1H, m, m-PyH), 7.10 (2H, m, p-PyH), 6.73 (2H, s, m-ArH), 5.97 (10H, s, Cp), 2.18 (3H, s, p-Ar-CH_3), 1.79 (6H, s, o-Ar-CH_3) ppm. ^{15}N-HMBC NMR (500 MHz, 51 MHz, PhBr-d_5) signal not seen for FLP (see Results and Discussion). NB: pyridine δ = 318.9 ppm.

1d. ^{1}H NMR (500 MHz, PhBr-d_5) δ 8.62 (1H, br, o-PyH), 7.96 (1H, m, p-PyH), 7.40 (2H, m, m-PyH), 6.74 (2H, s, m-ArH), 5.99 (10H, s, Cp), 2.18 (3H, s, p-Ar-CH_3), 2.11 (3H, br, o-Py-CH_3), 1.83 (6H, s, o-Ar-CH_3) ppm. ^{15}N-HMBC NMR (500 MHz, 51 MHz, PhBr-d_5) δ 302.1 (Zr-$NC_5H_4CH_3$) ppm. NB: 2-methylpyridine δ = 317.7 ppm.

1e. ^{1}H NMR (500 MHz, PhBr-d_5) δ 7.25 (1H, t, $^3J_{HH}$ = 7.7 Hz, p-PyH), 6.81 (2H, m, m-PyH), 6.71 (2H, s, m-ArH), 6.02 (10H, s, Cp), 2.27 (6H, s, o-Py-CH_3), 2.16 (3H, s, p-Ar-CH_3), 1.72 (6H, s, o-ArH-CH_3) ppm. ^{15}N-HMBC NMR (500 MHz, 51 MHz, PhBr-d_5) δ 249.8 (Zr-$NC_5H_3(CH_3)_2$) ppm. NB: 2,6-dimethylpyridine δ = 317.2 ppm.

$[Cp^*{}_2ZrOMes][B(C_6F_5)_4]$ // LB (2a−e). In a glovebox, 2 (34.1 mg, 0.029 mmol) was dissolved in bromobenzene-d_5 (0.5 mL) before the Lewis base (a = NEt_3 (4.1 μL, 0.029 mmol), b = $^iPr_2NEt$ (5.1 μL, 0.029 mmol), c = pyridine (2.4 μL, 0.029 mmol), d = 2-methylpyridine (2.9 μL, 0.029 mmol), e = 2,6-dimethylpyridine (3.4 μL, 0.029 mmol)) was added. A color change (dark orange to red) was observed for a, b, and e. The solution turned green upon addition of c, and slightly lightened in color upon addition of d.

The FLP was then used in situ for reactions with substrates, without isolation. However, crystals of 2c and 2d suitable for X-ray crystallography were obtained by layering a PhCl solution of 2c, and a PhBr-d_5 solution of 2d with pentane.

2a. ^{1}H NMR (500 MHz, PhCl-d_5) δ 6.79 (2H, s, m-ArH), 2.37 (6H, q, $^3J_{HH}$ = 7.2 Hz, $N(CH_2CH_3)_3$), 2.20 (3H, s, p-Ar-CH_3), 1.73 (6H, s, o-Ar-CH_3), 1.64 (30H, s, Cp*), 0.82 (9H, t, $^3J_{HH}$ = 7.2 Hz, $N(CH_2CH_3)_3$) ppm. ^{15}N-HMBC NMR (500 MHz, 51 MHz, PhBr-d_5) δ 54.2 (Zr-NEt_3) ppm. NB: NEt_3 δ = 47.6 ppm.

2b. ^{1}H NMR (500 MHz, PhBr-d_5) δ 6.78 (2H, s, m-ArH), 2.91 (2H, sept., $^3J_{HH}$ = 6.5 Hz, $N(CH(CH_3)_2)_2$), 2.37 (2H, q, $^3J_{HH}$ = 7.2 Hz, NCH_2CH_3), 2.20 (3H, s, p-Ar-CH_3), 1.73 (6H, s, o-Ar-CH_3), 1.64 (30H, s, Cp*), 1.05−0.63 (15H, br, $CH_3CH_2N(CH(CH_3)_2)_2$) ppm. ^{15}N-HMBC NMR (500 MHz, 51 MHz, PhBr-d_5) signal not seen for FLP (see Results and Discussion).

2c. ^{1}H NMR (500 MHz, PhBr-d_5) δ 8.55 (1H, br, o-ArH), 8.38 (1H, br, o-ArH), 7.32 (1H, br, p-ArH), 7.07−6.97 (2H, m, m-ArH(Py)), 6.78 (1H, s, m-ArH(Mes)), 6.67 (1H, s, m-ArH(Mes)), 2.17 (3H, s, p-Ar-CH_3), 1.94 (3H, s, o-Ar-CH_3), 1.89 (3H, s, o-Ar-CH_3), 1.47 (30H, s, Cp*) ppm. ^{13}C NMR (125 MHz, PhBr-d_5) δ 156.4 (s, i-C), 151.7 (s, o-CH(Py)), 138.2 (s, p-CH(Py)), 130.7 and 130.2 (s, m-CH(Mes)), 126.5 (s, o-CCH_3(Mes)), 125.8 (s, Cp*), 123.6 (s, p-CCH_3(Mes)), 21.7 and 20.4 (s, o-CH_3), 19.42 (s, p-CH_3), 11.5 (s, Cp*-Me) ppm. Remaining peaks obscured by PhBr-d_5 solvent. ^{15}N-HMBC NMR (500 MHz, 51 MHz, PhBr-d_5) δ 260.5 (Zr-Py) ppm. NB: Pyridine δ = 318.9 ppm. ESI-MS (+ve detection) 574.2645 m/z.

2d. ^{1}H NMR (500 MHz, PhBr-d_5) δ 7.94 (1H, br, o-ArH), 7.41 (1H, m, p-ArH), 7.16−7.12 (2H, m, m-ArH(Py)), 6.73 and 6.71 (2H, s, m-ArH(Mes)), 2.20 (3H, s, o-Ar-CH_3(Py)), 2.16 (3H, s, p-Ar-CH_3), 1.99 (3H, s, o-Ar-CH_3(Mes)), 1.78 (3H, s, o-Ar-CH_3(Mes)), 1.51 (30H, s, Cp*) ppm. ^{13}C NMR (125 MHz, PhBr-d_5) δ 155.8 (s, o-CCH_3(Py)), 148.4 (s, o-CH(Py)), 134.2 (s, p-CH(Py)), 128.6 (s, Cp*), 26.1 (s, o-CH_3(Py)), 20.8 and 20.4 (s, o-CH_3(Mes)), 19.3 (s, p-CH_3), 12.0 (s, Cp*-Me) ppm. Remaining peaks obscured by PhBr-d_5 solvent. ^{15}N-HMBC NMR (500 MHz, 51 MHz, PhBr-d_5) δ 261.1 (Zr-$NC_5H_4(CH_3)$) ppm. NB: 2-methylpyridine δ = 317.7 ppm.

2e. ^{1}H NMR (500 MHz, PhBr-d_5) δ 7.23 (1H, t, $^3J_{HH}$ = 7.8 Hz, p-PyH), 6.79 (2H, s, m-ArH), 6.72 (2H, m, m-PyH), 2.30 (6H, s, o-Py-CH_3), 2.20 (3H, s, p-Ar-CH_3), 1.73 (6H, s, o-Ar-CH_3), 1.63 (30H, s, Cp*) ppm. ^{15}N-HMBC NMR (500 MHz, 51 MHz, PhBr-d_5) δ 286.0 (Zr-$NC_5H_3(CH_3)_2$) ppm. NB: 2,6-dimethylpyridine δ = 317.2 ppm.

DOSY Studies of 1a−e and 2a−e. Samples of 1a−e and 2a−e and separate control samples of a-e were made as detailed above. ^{1}H DOSY NMR spectroscopy was carried out using 15 increments and a diffusion delay of 100 ms. The results of the study can be found in the Supporting Information. All data were analyzed using MestReNova.

Reactions of Pairs with D_2. Reactivity of [$Cp_2ZrOMes$][$B(C_6F_5)_4$] // LB (1a−e). In a glovebox, **1** (30 mg, 0.029 mmol) was dissolved in PhCl (0.5 mL) in an NMR tube fitted with a J. Youngs valve, before C_6D_6 (one drop) was added for reference in ^{2}H NMR spectra. An equimolar amount of the Lewis base (**a** = NEt_3 (4.1 μL, 0.029 mmol), **b** = ^{i}Pr_2NEt (5.1 μL, 0.029 mmol), **c** = pyridine (2.4 μL, 0.029 mmol), **d** = 2-methylpyridine (2.9 μL, 0.029 mmol), **e** = 2,6-dimethylpyridine (3.4 μL, 0.029 mmol)) was then added. Outside of the glovebox, the sample was degassed twice via freeze−pump−thaw, before being refilled with D_2 gas (1 bar). In all cases, no change in the NMR spectra was seen.

Reactivity of [$Cp^*{}_2ZrOMes$][$B(C_6F_5)_4$] // LB (2a−e). In a glovebox, **2** (34.1 mg, 0.029 mmol) was dissolved in PhCl (0.5 mL) in an NMR tube fitted with a J. Youngs valve, before C_6D_6 (one drop) was added for reference in ^{2}H NMR spectra. An equimolar amount of the Lewis base (**a** = NEt_3 (4.1 μL, 0.029 mmol), **b** = ^{i}Pr_2NEt (5.1 μL, 0.029 mmol), **c** = pyridine (2.4 μL, 0.029 mmol), **d** = 2-methylpyridine (2.9 μL, 0.029 mmol), **e** = 2,6-dimethylpyridine (3.4 μL, 0.029 mmol)) was then added. Outside of the glovebox, the sample was degassed twice via freeze−pump−thaw, before being refilled with D_2 gas (1 bar). A color change from red to yellow was seen for **2a**, **2b**, and **2e**. Collected spectral data are detailed below:

2a + D_2. ^{2}H NMR (77 MHz, PhCl/C_6D_6) δ 6.06 (s, Zr-D) ppm.

2b + D_2. ^{2}H NMR (77 MHz, PhCl/C_6D_6) δ 6.06 (s, Zr-D) ppm.

2e + D_2. ^{2}H NMR (77 MHz, PhCl/C_6D_6) δ 12.4 (br, N-D), 6.06 (s, Zr-D) ppm.

Reactions of Pairs with CO_2. Reactivity of [$Cp_2ZrOMes$][$B(C_6F_5)_4$] // LB (1a−e). In a glovebox, **1** (30 mg, 0.029 mmol) was dissolved in PhBr-d_5 (0.5 mL) in an NMR tube fitted with a J. Youngs valve. An equimolar amount of the Lewis base (**a** = NEt_3 (4.1 μL, 0.029 mmol), **b** = ^{i}Pr_2NEt (5.1 μL, 0.029 mmol), **c** = pyridine (2.4 μL, 0.029 mmol), **d** = 2-methylpyridine (2.9 μL, 0.029 mmol), **e** = 2,6-dimethylpyridine (3.4 μL, 0.029 mmol)) was then added. Outside of the glovebox, the sample was degassed twice via freeze−pump− thaw, before being refilled with CO_2 gas (1 bar) via a −78 °C trap. **1a**, **1b**, and **1d** showed a lightening in color, whereas **1e** showed no clear color change. Isolation of any products was attempted but not possible, and so all spectral data were obtained in situ. **1c** did not react.

1a + CO_2. ^{1}H NMR (500 MHz, PhBr-d_5) δ 6.85 (2H, s, m-ArH), 6.17 (10H, s, Cp), 2.37 (6H, q, $N(CH_2CH_3)_3$), 2.28 (3H, s, p-Ar-CH_3), 2.23 (6H, s, o-Ar-CH_3), 0.80 (9H, t, $N(CH_2CH_3)_3$) ppm. ^{13}C NMR (125 MHz, PhBr-d_5) δ 165.3 (s, C(O) O), 161.8 (s, i-C), 128.6 (s, o-C), 126.5 (s, m-C), 124.6 (s, p-C), 112.9 (s, Cp), 47.0 (s, $N(CH_2CH_3)_3$), 20.9 (s, p-CH_3), 18.6 (s, o-CH_3), 10.5 (s, $N(CH_2CH_3)_3$) ppm. ^{15}N-HMBC NMR (500 MHz, 51 MHz, PhBr-d_5) δ 446.0 (Zr-CO_2-NEt_3) ppm.

1b + CO_2. ^{1}H NMR (500 MHz, PhBr-d_5) δ 6.85 (2H, s, m-ArH), 6.17 (10H, s, Cp), 2.92 (2H, sept., $N(CH(CH_3)_2)_2$), 2.38 (2H, q, NCH_2CH_3), 2.28 (3H, s, p-Ar-CH_3), 2.23 (6H, s, o-Ar-CH_3), 1.00−0.65 (15H, br, $CH_3CH_2N(CH(CH_3)_2)_2$) ppm. ^{13}C NMR (125 MHz, PhBr-d_5) δ 168.2 (s, C(O) O), 161.8 (s, i-C), 128.6 (s, o-C), 126.5 (s, m-C), 124.7 (s, p-C), 112.9 (s, Cp), 56.0 $N(CH(CH_3)_2)_2$), 43.4 (s, NCH_2CH_3), 21.0 (s, $N(CH(CH_3)_2)_2$), 20.7 (s, p-CH_3), 18.7 (s, o-CH_3), 16.6 (s, NCH_2CH_3) ppm. ^{15}N-HMBC NMR (500 MHz, 51 MHz, PhBr-d_5) δ 446.5 (Zr-CO_2-N(^{i}Pr)$_2$Et) ppm.

1d + CO_2. ^{1}H NMR (500 MHz, PhBr-d_5) δ 8.62 (1H, br, o-PyH), 7.82 (1H, m, p-PyH), 7.44 (2H, m, m-PyH), 6.85 (2H, s, m-ArH), 6.17 (10H, s, Cp), 2.28 (3H, s, p-Ar-CH_3), 2.17 (6H, s, o-Ar-CH_3), 2.10 (3H, br, o-Py-CH_3) ppm. ^{13}C NMR (125 MHz, PhBr-d_5) δ 161.6 (s, C(O) O), 160.9 (s, i-C), 155.0 (s, o-CCH_3(Py)), 142.5 (s, o-CH(Py)), 134.0 (s, p-C(Py)), 128.4 (s, o-C(Mes)), 126.3 (s, m-C(Mes)), 124.7 (s, p-C(Mes)), 124.4 (s, m-C(Py)), 123.0 (s, m-C(Py)), 112.7 (s, Cp), 25.4 (s, o-CH_3(Py)), 20.6 (s, p-CH_3), 18.4 (s, o-CH_3(Mes)) ppm. ^{15}N-HMBC NMR (500 MHz, 51 MHz, PhBr-d_5) δ 450.1 (Zr-CO_2-$NC_5H_4CH_3$) ppm.

1e + CO_2. ^{1}H NMR (500 MHz, PhBr-d_5) δ 7.33 (1H, t, $^3J_{HH}$ = 7.7 Hz, p-PyH), 6.79 (2H, m, m-PyH), 6.74 (2H, s, m-ArH), 6.14 (10H, s, Cp), 2.37 (3H, s, p-Ar-CH_3), 2.15 (6H, s, o-ArH-CH_3) 2.12 (6H, s, o-Py-CH_3), ppm. ^{13}C NMR (125 MHz, PhBr-d_5) 160.9 (s, C(O) O), 160.5 (s, i-C), 155.4 (s, o-C(Py)), 140.0 (s, p-C(Py)), 128.6 (s, o-C(Mes)), 126.5 (s, m-C(Mes)), 124.7 (s, p-C(Mes)), 115.6 (s, Cp), 34.2 (s, o-CH_3(Py)), 21.6 (s, p-CH_3), 17.7 (s, o-CH_3(Mes)) ppm. Remaining peaks obscured by PhBr-d_5 solvent. ^{15}N-HMBC NMR (500 MHz, 51 MHz, PhBr-d_5) δ 464.0 (Zr-CO_2-$NC_5H_3(CH_3)_2$) ppm.

Reactivity of [$Cp^*{}_2ZrOMes$][$B(C_6F_5)_4$] // LB (2a−e). In a glovebox, **2** (34.1 mg, 0.029 mmol) was dissolved in PhBr-d_5 (0.5 mL) in an NMR tube fitted with a J. Youngs valve. An equimolar amount of the Lewis base (**a** = NEt_3 (4.1 μL, 0.029 mmol), **b** = ^{i}Pr_2NEt (5.1 μL, 0.029 mmol), **c** = pyridine (2.4 μL, 0.029 mmol), **d** = 2-methylpyridine (2.9 μL, 0.029 mmol), **e** = 2,6-dimethylpyridine (3.4 μL, 0.029 mmol)) was then added. Outside of the glovebox, the sample was degassed twice via freeze−pump−thaw, before being refilled with CO_2 gas (1 bar) via a −78 °C. A color change from to yellow was seen for **2a**, **2b**, **2d**, and **2e**. Isolation of any products was attempted but not possible, and so all spectral data were obtained in situ. **2c** did not react.

2a + CO_2. ^{1}H NMR (500 MHz, PhBr-d_5) δ 6.71 (2H, s, m-ArH), 2.33 (6H, q, $N(CH_2CH_3)_3$), 2.15 (3H, s, p-Ar-CH_3), 1.94 (6H, s, o-Ar-CH_3), 1.83 (30H, s, Cp*), 0.75 (9H, t, $N(CH_2CH_3)_3$) ppm. ^{13}C NMR (125 MHz, PhCl) δ 162.7 (s, C(O) O), 156.7 (s, i-C), 124.6 (s, o-C), 123.2 (s, p-C), 121.7 (s, Cp*), 46.9 (s, $N(CH_2CH_3)_3$), 20.3 (s, p-CH_3), 16.9 (s, o-CH_3), 10.9 (s, $N(CH_2CH_3)_3$), 9.4 (s, Cp*) ppm. ^{15}N-HMBC NMR (500 MHz, 51 MHz, PhBr-d_5) δ 343.3 (Zr-CO_2-NEt_3) ppm.

2b + CO_2. ^{1}H NMR (500 MHz, PhBr-d_5) δ 6.80 (2H, s, m-ArH), 2.91 (2H, br, $N(CH(CH_3)_2)_2$), 2.38 (2H, q, $^3J_{HH}$ = 7.2 Hz, NCH_2CH_3), 2.16 (3H, s, p-Ar-CH_3), 1.90 (6H, s, o-Ar-CH_3), 1.83 (30H, s, Cp*), 1.00−0.74 (15H, br, $CH_3CH_2N(CH(CH_3)_2)_2$) ppm. ^{13}C NMR (125 MHz, PhBr-d_5) δ 161.4 (s, C(O) O), 155.9 (s, i-C), 124.7 (s, o-C), 123.1 (s, p-C), 56.1 (s, $N(CH(CH_3)_2)_2$), 43.5 (s, NCH_2CH_3), 21.1 (s, $N(CH(CH_3)_2)_2$), 22.6 (s, p-CH_3), 18.4 (s, o-CH_3), 16.7 (s, NCH_2CH_3), 11.3 (s, Cp*) ppm. Remaining NMR peaks obscured by solvent. ^{15}N-HMBC NMR (500 MHz, 51 MHz, PhBr-d_5) signal not seen (see Results and Discussion).

2d + CO_2. ^{1}H NMR (500 MHz, PhBr-d_5) δ 7.65 (1H, m, p-PyH), 7.47 (1H, m, m-PyH), 6.97−6.90 (2H, m, Py), 6.52 (2H, s, m-ArH), 6.17 (10H, s, Cp), 2.22 (3H, s, p-Ar-CH_3), 2.16 (3H, br, o-Py-CH_3), 1.88 (30H, s, Cp*), 1.75 (6H, s, o-Ar-CH_3), ppm. ^{15}N-HMBC NMR (500 MHz, 51 MHz, PhBr-d_5) δ 438.1 (Zr-CO_2-$NC_5H_4CH_3$) ppm.

2e + CO_2. ^{1}H NMR (500 MHz, PhBr-d_5) δ 7.30 (1H, t, $^3J_{HH}$ = 7.8 Hz, p-PyH), 6.80 (2H, s, m-ArH), 6.74 (2H, m, m-PyH), 2.18 (6H, s, o-Py-CH_3), 1.89 (3H, s, p-Ar-CH_3), 1.81 (30H, s, Cp*), 1.76 (6H, s, o-Ar-CH_3) ppm. ^{15}N-HMBC NMR (500 MHz, 51 MHz, PhBr-d_5) δ 466.1 (Zr-CO_2-$NC_5H_3(CH_3)_2$) ppm.

Reactions of Pairs with Tetrahydrofuran (THF). Reactivity of [$Cp_2ZrOMes$][$B(C_6F_5)_4$] // LB (1a−e). In a glovebox, **1** (30 mg, 0.029 mmol) was dissolved in PhBr-d_5 (0.5 mL) in an NMR tube fitted with a J. Youngs valve. An equimolar amount of the Lewis base (**a** = NEt_3 (4.1 μL, 0.029 mmol), **b** = ^{i}Pr_2NEt (5.1 μL, 0.029 mmol), **c** = pyridine (2.4 μL, 0.029 mmol), **d** = 2-methylpyridine (2.9 μL, 0.029 mmol), **e** = 2,6-dimethylpyridine (3.4 μL, 0.029 mmol)) was then added. Tetrahydrofuran (THF, 2.4 μL, 0.029 mmol) was then added, with **1a**, **1b**, **1d**, and **1e** all forming yellow solutions (already yellow solutions darkened slightly). **1a** was left to react at room temperature for 24 h; all other reactions were heated to 80 °C for 3 days. Where sufficient quantities of product were present, the sample was precipitated out into stirring hexane, before being washed twice with hexane (2 × 1 mL) and once with pentane (1 mL) before being dried in vacuo.

1a + THF. Yield = 28.9 mg, 82%. ^{1}H NMR (400 MHz, PhBr-d_5): δ 6.80 (2H, s, Ar-H), 6.07 (10H, s, Cp), 3.90 (2H, m, α-CH_2), 2.50 (2H, m, δ-CH_2), 2.43 (6H, q, $^3J_{HH}$ = 7 Hz, $N(CH_2CH_3)_3$), 2.22 (3H, s, p-CH_3), 2.12 (6H, s, o-CH_3), 1.31 (4H, m, β-CH_2 and γ-CH_2), 0.68 (9H, m, $N(CH_2CH_3)_3$) ppm. ^{13}C NMR (125 MHz, PhBr-d_5): δ 161.0 (s, i-C), 127.4 (s, o-C), 124.6 (s, p-C), 112.8 (s, Cp), 71.9 (s, α-CH_2), 48.1 (s, β-CH_2), 30.5 (s, γ-CH_2), 20.8 (s, p-CH_3), 18.5 (s, δ-CH_2), 17.9 (s, o-CH_3), 11.8 (s, $N(CH_2CH_3)$), 6.73 (s, $N(CH_2CH_3)$) ppm.

Remaining peaks obscured by PhBr-d_5 solvent. ^{15}N-HMBC NMR (500 MHz, 51 MHz, PhBr-d_5): δ 337.5 (-CH_2NEt_3) ppm. ESI-MS (+ve detection) 528.2422 m/z $[M]^+$, 174.1930 m/z $[HO(C_4H_8)\text{-}NEt_3]^+$.

1b + THF. Yield = 17% (by NMR). Not enough product to isolate. ^{15}N-HMBC (500 MHz, 51 MHz, PhBr-d_5): δ 315.8 ppm. ESI-MS (+ve detection) 556.2742 m/z $[M]^+$, 202.2217 m/z $[HO(C_4H_8)N(^iPr)_2Et]^+$.

1d + THF. Yield = 15.8 mg, 45%. ^{1}H NMR (400 MHz, PhBr-d_5): δ 7.65 (1H, m, o-ArH), 7.50−7.39 (1H, m, p-ArH), 6.99−6.86 (2H, m, m-ArH(Py)), 6.80 (2H, s, Ar-H(Mes)), 6.05 (10H, s, Cp), 3.93−3.85 (4H, m, α-CH_2 and δ-CH_2), 2.23 (3H, s, p-CH_3), 2.17 (3H, s, o-CH_3(Py)), 2.09 (6H, s, o-CH_3), 1.65 (2H, m, β-CH_2), 1.35 (2H, m, γ-CH_2) ppm. ^{13}C NMR (125 MHz, PhBr-d_5): δ 160.1 (s, i-C(Mes)), 154.6 (s, o-CCH_3(Py)), 141.5 (s, p-CH(Py)), 127.4 (s, o-CCH_3(Mes)), 125.6 (s, m-CH(Py)), 124.6 (s, p-CCH_3(Mes)), 123.6 (s, m-CH(Py)), 112.8 (s, Cp), 72.0 (s, α-CH_2), 34.3 (s, β-CH_2), 30.3 (s, γ-CH_2), 27.3 (s, o-CH_3(Py)), 20.8 (s, p-CH_3(Mes)), 19.4 (s, δ-CH_2), 17.9 (s, o-CH_3(Mes)) ppm. Remaining aromatic peaks obscured by PhBr-d_5 solvent. ^{15}N-HMBC NMR (500 MHz, 51 MHz, PhBr-d_5): δ 411.6 ppm. ESI-MS (+ve detection) 520.1796 m/z $[M]^+$, 166.1275 m/z $[HO(C_4H_8)N(CH_3)C_6H_4]^+$.

1e + THF. Yield = 23 mg, 65%. ^{1}H NMR (400 MHz, PhBr-d_5): δ 7.37 (1H, t, $^3J_{HH}$ = 8 Hz, p-ArH), 6.82−6.72 (2H, m, m-ArH(Py)), 6.80 (2H, s, Ar-H(Mes)), 6.05 (10H, s, Cp), 3.93 (2H, t, $^3J_{HH}$ = 6 Hz, α-CH_2), 3.85 (2H, m, δ-CH_2), 2.26 (6H, s, o-CH_3(Py)), 2.23 (3H, s, p-CH_3), 2.10 (6H, s, o-CH_3), 1.58 (2H, m, β-CH_2), 1.45 (2H, m, γ-CH_2) ppm. ^{13}C NMR (125 MHz, PhBr-d_5): δ 161.0 (s, i-C(Mes)), 154.3 (s, o-CCH_3(Py)), 143.8 (s, p-CH(Py)), 127.4 (s, o-CCH_3(Mes)), 124.6 (s, p-CCH_3(Mes)), 124.0 (s, m-CH(Py)), 112.8 (s, Cp), 71.8 (s, α-CH_2), 34.3 (s, β-CH_2), 30.7 (s, γ-CH_2), 25.6 (s, o-CH_3(Py)), 20.8 (s, p-CH_3(Mes)), 19.8 (s, δ-CH_2), 17.9 (s, o-CH_3(Mes)) ppm. Remaining aromatic peaks obscured by PhBr-d_5 solvent. ^{15}N-HMBC (500 MHz, 51 MHz, PhBr-d_5): δ 411.8 ppm. ESI-MS (+ve detection) 534.1938 m/z $[M]^+$, 180.1436 m/z $[HO(C_4H_8)N(CH_3)_2C_6H_3]^+$.

Reactivity of $[Cp^*_2ZrOMes][B(C_6F_5)_4]$ // LB (2a−e). In a glovebox, 2 (34 mg, 0.029 mmol) was dissolved in PhBr-d_5 (0.5 mL) in an NMR tube fitted with a J. Youngs valve. An equimolar amount of the Lewis base (a = NEt_3 (4.1 μL, 0.029 mmol), b = $^iPr_2NEt$ (5.1 μL, 0.029 mmol), c = pyridine (2.4 μL, 0.029 mmol), d = 2-methylpyridine (2.9 μL, 0.029 mmol), e = 2,6-dimethylpyridine (3.4 μL, 0.029 mmol)) was then added. Tetrahydrofuran (THF, 2.4 μL, 0.029 mmol) was then added, with 2a, 2d, and 2e all forming yellow solutions. The reactions were heated at 80 °C for 5 days. Isolation of the products was not possible.

2a + THF. Yield = 17% (by NMR). ^{15}N-HMBC (500 MHz, 51 MHz, PhBr-d_5): δ 341.4 ppm. ESI-MS (+ve detection) 668.3975 m/z $[M + H]^+$, 174.1888 m/z $[HO(C_4H_8)NEt_3]^+$.

2d + THF. Yield = 40% (by NMR). ^{15}N-HMBC (500 MHz, 51 MHz, PhBr-d_5): δ 411.3 ppm. ESI-MS (+ve detection) 660.3350 m/z $[M + H]^+$, 166.1277 m/z $[HO(C_4H_8)N(CH_3)C_6H_4]^+$.

2e + THF. Yield = 7% (by NMR). Too little product for ^{15}N-HMBC NMR. ESI-MS (+ve detection) 674.3501 m/z $[M + H]^+$, 180.1418 m/z $[HO(C_4H_8)N(CH_3)_2C_6H_3]^+$.

Reaction of Pairs with Phenylacetylene-d (PhCCD). Reactivity of $[Cp_2ZrOMes][B(C_6F_5)_4]$ // LB (1a−e). In a glovebox, 1 (30 mg, 0.029 mmol) was dissolved in PhBr-d_5 (0.5 mL) in an NMR tube fitted with a J. Youngs valve. An equimolar amount of the Lewis base (a = NEt_3 (4.1 μL, 0.029 mmol), b = $^iPr_2NEt$ (5.1 μL, 0.029 mmol), c = pyridine (2.4 μL, 0.029 mmol), d = 2-methylpyridine (2.9 μL, 0.029 mmol), e = 2,6-dimethylpyridine (3.4 μL, 0.029 mmol)) was then added. Excess phenylacetylene-d (3 drops) was then added, resulting in a lightening of the yellow color for 1a and 1b, with no color change seen for the reactions of 1c−e. Neither 1c nor 1d demonstrated any reactivity. The Zr-acetylide complex could not be isolated in any reaction, so the spectral data was obtained in situ.

$Cp_2Zr(OMes)CCPh$. ^{1}H NMR (500 MHz, PhBr-d_5) δ 7.53 (2H, m, o-ArH), 7.18 (3H, m, p-ArH & m-ArH(Ph)), 6.76 (2H, s, m-ArH(Mes)), 6.09 (10H, s, Cp), 2.21 (6H, s, o-Ar-CH_3), 2.19 (3H, s, p-Ar-CH_3) ppm.

1a + PhCCD. Mixture of products meant the Zr-acetylide complex could not be isolated. However, colorless crystals of $[D\text{-}NEt_3][B\text{-}(C_6F_5)_4]$ formed in solution, which were filtered, washed with PhCl (3 × 0.5 mL) and dried in vacuo. ^{15}N-HMBC NMR (500 MHz, 51 MHz, PhBr-d_5) δ 452.2 (D-NEt_3) ppm. ^{1}H (400 MHz, CD_3CN) δ 3.22 (6H, q, D-$N(CH_2CH_3)_3$), 1.22 (9H, t, D-$N(CH_2CH_3)_3$) ppm. Deuteride signal not visible in ^{2}H NMR spectrum due to solvent interactions. Nanospray (+ve detection) 103.1 m/z $[D\text{-}NEt_3]^+$.

1b + PhCCD. Mixture of products meant the Zr-acetylide complex could not be isolated. However, colorless crystals of $[D\text{-}N(^iPr)_2Et]\text{-}[B(C_6F_5)_4]$ formed in solution, which were filtered, washed with PhCl (3 × 0.5 mL) and dried in vacuo. ^{15}N-HMBC NMR (500 MHz, 51 MHz, PhBr-d_5) δ 424.8 (D-$N(^iPr)_2Et$) ppm. ^{1}H (400 MHz, CD_3CN) δ 3.67 (2H, sept., $N(CH(CH_3)_2)_2$), 3.15 (2H, q, NCH_2CH_3), 1.38−1.25 (15H, m, $N(CH(CH_3)_2)_2$ and NCH_2CH_3) ppm. Deuteride signal not visible in ^{2}H NMR spectrum due to solvent interactions. Nanospray (+ve detection) 131.2 m/z $[D\text{-}N(^iPr)_2Et]^+$.

1e + PhCCD. Mixture of products meant the Zr-acetylide complex could not be isolated. Spectral data shown for $[D\text{-}NC_5H_3(CH_3)_2]^+$. ^{15}N-HMBC NMR (500 MHz, 51 MHz, PhBr-d_5) δ 420.8 (D-$NC_5H_3(CH_3)_2$) ppm. ^{1}H NMR (400 MHz, CD_3CN) δ 7.85 (1H, t, p-ArH), 7.27 (2H, dd, m-ArH), 2.55 (6H, s, -CH_3) ppm. ^{2}H NMR (77 MHz, PhBr-d_5) δ 12.45 (br, D-$NC_5H_3(CH_3)_2$) ppm. Nanospray (+ve detection) 109.1 m/z $[D\text{-}NC_5H_3(CH_3)_2]^+$.

Reactivity of $[Cp^*_2ZrOMes][B(C_6F_5)_4]$ // LB (2a−e). In a glovebox, 2 (34.1 mg, 0.029 mmol) was dissolved in PhCl (0.5 mL) in an NMR tube fitted with a J. Youngs valve and C_6D_6 (one drop) was added as a reference in ^{2}H spectra. An equimolar amount of the Lewis base (a = NEt_3 (4.1 μL, 0.029 mmol), b = $^iPr_2NEt$ (5.1 μL, 0.029 mmol), c = pyridine (2.4 μL, 0.029 mmol), d = 2-methylpyridine (2.9 μL, 0.029 mmol), e = 2,6-dimethylpyridine (3.4 μL, 0.029 mmol)) was then added. Excess phenylacetylene-d (3 drops) was then added. Samples 2a and 2b turned yellow within 5 min. 2c did not demonstrate any reactivity. The Zr-acetylide complex could not be isolated in any reaction, so the spectral data was obtained in situ.

$Cp^*_2Zr(OMes)CCPh$. ^{1}H NMR (500 MHz, PhCl) δ 7.56 (2H, m, o-ArH), 6.69 (2H, s, m-ArH(Mes)), 2.16 (3H, s, p-Ar-CH_3), 1.88 (30H, s, Cp*), 1.79 (6H, s, o-Ar-CH_3) ppm. Remaining peaks were obscured by the PhCl solvent.

2a + PhCCD. Mixture of products meant the Zr-acetylide complex could not be isolated. However, colorless crystals of $[D\text{-}NEt_3][B\text{-}(C_6F_5)_4]$ formed in solution, which were filtered, washed with PhCl (3 × 0.5 mL) and dried in vacuo. ^{15}N-HMBC NMR (500 MHz, 51 MHz, PhCl/C_6D_6) δ 439.7 (D-NEt_3) ppm. ^{1}H (400 MHz, CH_3CN/ C_6D_6) δ 3.06 (6H, q, D-$N(CH_2CH_3)_3$), 1.22 (9H, t, D-$N(CH_2CH_3)_3$) ppm. Deuteride signal not visible in ^{2}H NMR spectrum due to solvent interactions. Nanospray (+ve detection) 103.1 m/z $[D\text{-}NEt_3]^+$.

2b + PhCCD. Mixture of products meant the Zr-acetylide complex could not be isolated. However, colorless crystals of $[D\text{-}N(^iPr)_2Et]\text{-}[B(C_6F_5)_4]$ formed in solution, which were filtered, washed with PhCl (3 × 0.5 mL) and dried in vacuo. ^{15}N-HMBC NMR (500 MHz, 51 MHz, PhCl/C_6D_6) signal not seen (see Results and Discussion). ^{1}H (400 MHz, CH_3CN/C_6D_6) δ 3.59 (2H, sept., $N(CH(CH_3)_2)_2$), 3.07 (2H, q, NCH_2CH_3), 1.33−1.25 (15H, m, $N(CH(CH_3)_2)_2$ and NCH_2CH_3) ppm. Deuteride signal not visible in ^{2}H NMR spectrum due to solvent interactions. Nanospray (+ve detection) 131.2 m/z $[D\text{-}N(^iPr)_2Et]^+$.

2d + PhCCD. Mixture of products meant the Zr-acetylide complex could not be isolated. Spectral data shown for $[D\text{-}NC_5H_4(CH_3)]^+$. ^{15}N-HMBC NMR (500 MHz, 51 MHz, PhCl/C_6D_6) δ 426.5 (D-$NC_5H_4(CH_3)$) ppm. ^{1}H NMR (400 MHz, PhCl/C_6D_6) δ 2.05 (3H, s, -CH_3) ppm, aromatic peaks obscured. ^{2}H NMR (77 MHz, PhCl/ C_6D_6) δ 12.38 (br, D-$NC_5H_4(CH_3)$) ppm. Nanospray (+ve detection) 95.1 m/z $[D\text{-}NC_5H_4(CH_3)]^+$.

2e + PhCCD. Mixture of products meant the Zr-acetylide complex could not be isolated. Spectral data shown for $[D\text{-}NC_5H_3(CH_3)_2]^+$. ^{15}N-HMBC NMR (500 MHz, 51 MHz, PhCl/C_6D_6) δ 421.6 (D-

$NC_5H_3(CH_3)_2$) ppm. ^1H NMR (400 MHz, CD_3CN) δ 7.85 (1H, t, p-ArH), 7.27 (2H, dd, m-ArH), 2.55 (6H, s, $-CH_3$) ppm. ^2H NMR (77 MHz, CD_3CN) δ 12.47 (br, D-$NC_5H_3(CH_3)_2$) ppm. Nanospray (+ve detection) 109.1 m/z [D-$NC_5H_3(CH_3)_2]^+$.

Catalytic Dehydrocoupling of $Me_2NH·BH_3$. Reactivity of $[Cp_2ZrOMes][B(C_6F_5)_4]$ // LB (1a−e). In a glovebox, 1 (18.7 mg, 0.018 mmol) and $Me_2NH·BH_3$ (10.6 mg, 0.18 mmol) were weighed into separate vials and dissolved in PhBr-d_5 (0.5 mL). The relevant Lewis base (a = NEt_3 (2.5 μL, 0.018 mmol), b = $^iPr_2NEt$ (3.2 μL, 0.018 mmol), c = pyridine (1.5 μL, 0.018 mmol), d = 2-methylpyridine (1.8 μL, 0.018 mmol), e = 2,6-dimethylpyridine (2.1 μL, 0.018 mmol)) was then added to 1. The two solutions were then combined, and the fully mixed solution was transferred to a quartz J. Youngs NMR tube before the relevant spectra were then collected. No reaction was seen for 1c; however, the relevant spectra for the reactions of 1a, 1b, 1d, and 1e can be found in the Supporting Information (Figures S16−S20).

Reactivity of $[Cp^*_2ZrOMes][B(C_6F_5)_4]$ // LB (2a−e). In a glovebox, 2 (21.2 mg, 0.018 mmol) and $Me_2NH·BH_3$ (10.6 mg, 0.18 mmol) were weighed into separate vials and dissolved in PhBr-d_5 (0.5 mL). The relevant Lewis base (a = NEt_3 (2.5 μL, 0.018 mmol), b = $^iPr_2NEt$ (3.2 μL, 0.018 mmol), c = pyridine (1.5 μL, 0.018 mmol), d = 2-methylpyridine (1.8 μL, 0.018 mmol), e = 2,6-dimethylpyridine (2.1 μL, 0.018 mmol)) was then added to 2. The two solutions were then combined, and the fully mixed solution was transferred to a quartz J. Youngs NMR tube before the relevant spectra were then collected (please see Supporting Information, Figures S21−S25).

Catalytic Dehydrocoupling of $Me_2NH·BH_3$ at 60 °C. The reactions were prepared for 1a, 1e, and 2e using the same method shown above, with the spectra then collected in an NMR spectrometer set to 60 °C. Please see the Supporting Information for the collected spectra (Figures S26−S31).

ASSOCIATED CONTENT

* Supporting Information

DOSY spectra for 1a−e and 2a−e, experimental procedures and analytical data (^{11}B NMR spectra and reaction profiles) for all catalytic reactions, crystallographic data for 2c and 2d (PDF)

Accession Codes

CCDC 1898435−1898436 contain the supplementary crystallographic data for this paper. These data can be obtained free of charge via www.ccdc.cam.ac.uk/data_request/cif, or by emailing data_request@ccdc.cam.ac.uk, or by contacting The Cambridge Crystallographic Data Centre, 12 Union Road, Cambridge CB2 1EZ, UK; fax: +44 1223 336033.

AUTHOR INFORMATION

Corresponding Author

*E-mail: wassd@cardiff.ac.uk.

ORCID

Duncan F. Wass: 0000-0002-0356-7067

Notes

The authors declare no competing financial interest.

ACKNOWLEDGMENTS

H.B.H. would like to acknowledge Dr. Paul Gates and the University of Bristol Mass Spectrometry Service for their assistance. The EPSRC Centre for Doctoral Training in Catalysis is thanked for funding (to H.B.H.).

REFERENCES

(1) Welch, G. C.; San Juan, R. R.; Masuda, J. D.; Stephan, D. W. Reversible, Metal-Free Hydrogen Activation. Science 2006, 314, 1124−1126.
(2) Stephan, D. W.; Erker, G. Frustrated Lewis Pair Chemistry: Development and Perspectives. Angew. Chem., Int. Ed. 2015, 54, 6400−6441.
(3) Stephan, D. W.; Erker, G. Frustrated Lewis Pairs: Metal-free Hydrogen Activation and More. Angew. Chem., Int. Ed. 2010, 49, 46− 76.
(4) Chapman, A. M.; Haddow, M. F.; Wass, D. F. Frustrated lewis pairs beyond the main group: synthesis, reactivity, and small molecule activation with cationic zirconocene-phosphinoaryloxide complexes. J. Am. Chem. Soc. 2011, 133, 18463−18478.
(5) Chapman, A. M.; Haddow, M. F.; Wass, D. F. Cationic Group 4 Metallocene-(o-Phosphanylaryl)oxido Complexes: Synthetic Routes to Transition-Metal Frustrated Lewis Pairs. Eur. J. Inorg. Chem. 2012, 2012, 1546−1554.
(6) Xu, X.; Kehr, G.; Daniliuc, C. G.; Erker, G. 1,1-Carbozirconation: Unusual Reaction of an Alkyne with a Methyl Zirconocene Cation and Subsequent Frustrated Lewis Pair Like Reactivity. Angew. Chem., Int. Ed. 2013, 52, 13629−13632.
(7) Xu, X.; Kehr, G.; Daniliuc, C. G.; Erker, G. Reactions of a Cationic Geminal Zr+/P Pair with Small Molecules. J. Am. Chem. Soc. 2013, 135, 6465−6476.
(8) Xu, X.; Kehr, G.; Daniliuc, C. G.; Erker, G. Formation of unsaturated vicinal Zr+/P frustrated Lewis pairs by the unique 1,1-carbozirconation reactions. J. Am. Chem. Soc. 2014, 136, 12431− 12443.
(9) Xu, X.; Kehr, G.; Daniliuc, C. G.; Erker, G. Frustrated Lewis Pair Behavior of [Cp2ZrOCR2CH2PPh2]+ Cations. Organometallics 2015, 34, 2655−2661.
(10) Normand, A. T.; Daniliuc, C. G.; Wibbeling, B.; Kehr, G.; Le Gendre, P.; Erker, G. Phosphido- and Amidozirconocene Cation-Based Frustrated Lewis Pair Chemistry. J. Am. Chem. Soc. 2015, 137, 10796−10808.
(11) Jian, Z.; Daniliuc, C. G.; Kehr, G.; Erker, G. Frustrated Lewis Pair vs Metal−Carbon σ-Bond Insertion Chemistry at an o-Phenylene-Bridged Cp_2Zr^+/PPh_2 System. Organometallics 2017, 36, 424−434.
(12) Neu, R. C.; Otten, E.; Lough, A.; Stephan, D. W. The synthesis and exchange chemistry of frustrated Lewis pair-nitrous oxide complexes. Chem. Sci. 2011, 2, 170−176.
(13) Metters, O. J.; Forrest, S. J. K.; Sparkes, H. A.; Manners, I.; Wass, D. F. Small Molecule Activation by Intermolecular Zr(IV)-Phosphine Frustrated Lewis Pairs. J. Am. Chem. Soc. 2016, 138, 1994−2003.
(14) Metters, O. J.; Flynn, S. R.; Dowds, C. K.; Sparkes, H. A.; Manners, I.; Wass, D. F. Catalytic Dehydrocoupling of Amine−Boranes using Cationic Zirconium(IV)−Phosphine Frustrated Lewis Pairs. ACS Catal. 2016, 6, 6601−6611.
(15) Clark, E. R.; Ingleson, M. J. N-Methylacridinium Salts: Carbon Lewis Acids in Frustrated Lewis Pairs for σ-Bond Activation and Catalytic Reductions. Angew. Chem., Int. Ed. 2014, 53, 11306−11309.
(16) Chernichenko, K.; Nieger, M.; Leskela, M.; Repo, T. Hydrogen activation by 2-boryl-N,N-dialkylanilines: a revision of Piers' ansa-aminoborane. Dalton Trans 2012, 41, 9029−9032.
(17) Chernichenko, K.; Kotai, B.; Papai, I.; Zhivonitko, V.; Nieger, M.; Leskela, M.; Repo, T. Intramolecular Frustrated Lewis Pair with the Smallest Boryl Site: Reversible H2 Addition and Kinetic Analysis. Angew. Chem., Int. Ed. 2015, 54, 1749−1753.
(18) Chernichenko, K.; Lindqvist, M.; Kotai, B.; Nieger, M.; Sorochkina, K.; Papai, I.; Repo, T. Metal-Free sp2-C−H Borylation as a Common Reactivity Pattern of Frustrated 2-Aminophenylboranes. J. Am. Chem. Soc. 2016, 138, 4860−4868.
(19) Binding, S. C.; Zaher, H.; Mark Chadwick, F.; O'Hare, D. Heterolytic activation of hydrogen using frustrated Lewis pairs containing tris(perfluorobiphenyl)borane. Dalton Trans 2012, 41, 9061−9066.

(20) Courtemanche, M.-A.; Rochette, E.; Legare, M.-A.; Bi, W.; Fontaine, F.-G. Reversible hydrogen activation by a bulky haloborane based FLP system. Dalton Transactions 2016, 45, 6129−6135.
(21) Iashin, V.; Chernichenko, K.; Papai, I.; Repo, T. Atom-Efficient Synthesis of Alkynylfluoroborates Using BF_3-Based Frustrated Lewis Pairs. Angew. Chem., Int. Ed. 2016, 55, 14146−14150.
(22) Korte, L. A.; Blomeyer, S.; Heidemeyer, S.; Nissen, J. H.; Mix, A.; Neumann, B.; Stammler, H.-G.; Mitzel, N. W. Intramolecular Lewis pairs with two acid sites - reactivity differences between P- and N-based systems. Dalton Trans 2016, 45, 17319−17328.
(23) Li, H.; Wen, M.; Lu, G.; Wang, Z.-X. Catalytic metal-free intramolecular hydroaminations of non-activated aminoalkenes: A computational exploration. Dalton Trans 2012, 41, 9091−9100.
(24) Liu, L.; Vankova, N.; Heine, T. A kinetic study on the reduction of CO_2 by frustrated Lewis pairs: from understanding to rational design. Phys. Chem. Chem. Phys. 2016, 18, 3567−3574.
(25) Maier, A. F. G.; Tussing, S.; Schneider, T.; Flörke, U.; Qu, Z.-W.; Grimme, S.; Paradies, J. Frustrated Lewis Pair Catalyzed Dehydrogenative Oxidation of Indolines and Other Heterocycles. Angew. Chem., Int. Ed. 2016, 55, 12219−12223.
(26) Theuergarten, E.; Schlosser, J.; Schluns, D.; Freytag, M.; Daniliuc, C. G.; Jones, P. G.; Tamm, M. Fixation of carbon dioxide and related small molecules by a bifunctional frustrated pyrazolylborane Lewis pair. Dalton Trans 2012, 41, 9101−9110.
(27) von Wolff, N.; Lefevre, G.; Berthet, J. C.; Thuery, P.; Cantat, T. Implications of CO_2 Activation by Frustrated Lewis Pairs in the Catalytic Hydroboration of CO_2: A View Using N/Si+ Frustrated Lewis Pairs. ACS Catal. 2016, 6, 4526−4535.
(28) Yepes, D.; Jaque, P.; Fernandez, I. Deeper Insight into the Factors Controlling H_2 Activation by Geminal Aminoborane-Based Frustrated Lewis Pairs. Chem. - Eur. J. 2016, 22, 18801−18809.
(29) Yepes, D.; Jaque, P.; Fernandez, I. Hydrogenation of Multiple Bonds by Geminal Aminoborane-Based Frustrated Lewis Pairs. Chem. - Eur. J. 2018, 24, 8833−8840.
(30) Zhang, Y.; Miyake, G. M.; John, M. G.; Falivene, L.; Caporaso, L.; Cavallo, L.; Chen, E. Y. X. Lewis pair polymerization by classical and frustrated Lewis pairs: acid, base and monomer scope and polymerization mechanism. Dalton Trans 2012, 41, 9119−9134.
(31) Flynn, S. R.; Metters, O. J.; Manners, I.; Wass, D. F. Zirconium-Catalyzed Imine Hydrogenation via a Frustrated Lewis Pair Mechanism. Organometallics 2016, 35, 847−850.
(32) Linnell, R. Notes- Dissociation Constants of 2-Substituted Pyridines. J. Org. Chem. 1960, 25, 290−290.
(33) Fujii, T.; Nishida, H.; Abiru, Y.; Yamamoto, M.; Kise, M. Studies on Synthesis of the Antibacterial Agent NM441. II. Selection of a Suitable Base for Alkylation of 1-Substituted Piperazine with 4-(Bromomethyl)-5-methyl-1, 3-dioxol-2-one. Chem. Pharm. Bull. 1995, 43, 1872−1877.
(34) Matos, J. M. E.; Lima-Neto, B. S. Acyclic amines as ancillary ligands in Ru-based catalysts for ring-opening metathesis polymerization: Probing the electronic and steric aspects of cyclic and acyclic amines. J. Mol. Catal. A: Chem. 2006, 259, 286−291.
(35) Clarke, K.; Rothwell, K. 377. A kinetic study of the effect of substituents on the rate of formation of alkylpyridinium halides in nitromethane solution. J. Chem. Soc. 1960, 1885−1895.
(36) Rosorius, C.; Kehr, G.; Fröhlich, R.; Grimme, S.; Erker, G. Electronic Control of Frustrated Lewis Pair Behavior: Chemistry of a Geminal Alkylidene-Bridged Per-pentafluorophenylated P/B Pair. Organometallics 2011, 30, 4211−4219.
(37) Liedtke, R.; Fröhlich, R.; Kehr, G.; Erker, G. Frustrated Lewis Pair Reactions With Bis-Acetylenic Substrates: Exploring the Narrow Gap Separating Very Different Competing Reaction Pathways. Organometallics 2011, 30, 5222−5232.
(38) Rosorius, C.; Daniliuc, C. G.; Fröhlich, R.; Kehr, G.; Erker, G. Structural features and reactions of a geminal frustrated phosphane/borane Lewis pair. J. Organomet. Chem. 2013, 744, 149−155.
(39) Rosorius, C.; Möricke, J.; Wibbeling, B.; McQuilken, A. C.; Warren, T. H.; Daniliuc, C. G.; Kehr, G.; Erker, G. Frustrated Lewis Pair Chemistry Derived from Bulky Allenyl and Propargyl Phosphanes. Chem. - Eur. J. 2016, 22, 1103−1113.
(40) Elmer, L.-M.; Kehr, G.; Daniliuc, C. G.; Siedow, M.; Eckert, H.; Tesch, M.; Studer, A.; Williams, K.; Warren, T. H.; Erker, G. The Chemistry of a Non-Interacting Vicinal Frustrated Phosphane/Borane Lewis Pair. Chem. - Eur. J. 2017, 23, 6056−6068.
(41) Bush, R. C.; Angelici, R. J. Phosphine basicities as determined by enthalpies of protonation. Inorg. Chem. 1988, 27, 681−686.
(42) Chapman, A. M.; Haddow, M. F.; Wass, D. F. Frustrated Lewis Pairs beyond the Main Group: Cationic Zirconocene-Phosphino-aryloxide Complexes and Their Application in Catalytic Dehydrogen-ation of Amine Boranes. J. Am. Chem. Soc. 2011, 133, 8826−8829.